

The Sensitivity of Higgs Factories to Composite Higgs Models via Precision Measurements

Kamal Maayergi, Devin G. E. Walker

*Department of Physics and Astronomy, Dartmouth College
Hanover, NH 03755 USA*

Ora Cullen

*Department of Physics and Astronomy, Dartmouth College
Hanover, NH 03755 USA and
School of Mathematics, Trinity College Dublin, Ireland*

Michael E. Peskin

*SLAC National Accelerator Laboratory
Stanford University
Menlo Park, California 94025 USA*

We investigate the potential of precision Higgs factory measurements to discover signatures of a representative model of electroweak symmetry breaking in which the Higgs boson arises as a composite Nambu-Goldstone boson. In this model, as in other models of the “Little Higgs” or Natural Composite Higgs type, the primary perturbations of the Standard Model come from effects of vectorlike top quark partners. We carry out an explicit calculation of the Higgs potential in this model. Applying phenomenological constraints, we are left with a 3-dimensional parameter space. We then present results from a complete scan of this parameter space. The region in which significant departures from the Standard Model predictions extends to models in which the lightest top quark partner has a mass above 3 TeV. Little Higgs models with such heavy top partners also predict significant deviations from the Standard Model in the top quark electroweak couplings, in particular, in the model studied here, in the t_L coupling to the Z boson.

I. INTRODUCTION

The Higgs boson was discovered in 2012 [1, 2] at the Large Hadron Collider (LHC). Since then, the two main experiments focused on probing the couplings of the Higgs to vector bosons and fermions have been ATLAS and CMS [3, 4]. The results to date have all been consistent with the predictions for the unique Higgs boson of the Standard Model (SM), with coupling measurements achieving accuracies at the 10%–20% level for the W and Z bosons and the third-generation quarks and leptons. The consistency of these results with the theoretical predictions has firmly established the 125 GeV Higgs boson as the main source of spontaneous electroweak symmetry breaking. The High-Luminosity run of the LHC (HL-LHC) is an upgrade, currently underway, that will sharpen this picture by increasing the precision of coupling measurements to the 1–4% level; and extending the search for additional fermions beyond the 1 TeV mass scale [3].

Despite the great success of the LHC and its findings, questions still remain in our understanding, namely, the nature of the Higgs boson and the mechanism of electroweak symmetry breaking. In the SM, electroweak symmetry breaking is an assumption, implemented by the choice of input parameters. Moreover, the SM does not explain the large hierarchy of fermion masses, with ratios exceeding 100,000 between the heaviest and lightest fermions. It is therefore crucial to obtain new insights into the properties and possible partners of the 125 GeV

Higgs boson. This motivation has led to proposals for new e^+e^- colliders designed as “Higgs factories” to enable higher-precision measurements of the known Higgs boson h [4]. The hope is that precision measurements on the Higgs boson can give insight into its possible partners and new interactions. The top quark often plays a role in models of electroweak symmetry breaking, and so precision studies of the top quark are also part of this story. This paper will concentrate on a class of models of electroweak symmetry breaking in which the top quark plays an essential role.

Current proposals for Higgs factories now under consideration include the ILC [5] in Japan, the CEPC in China [6], and the FCC-ee and LCF at CERN [7, 8]. The projected precision for Higgs boson coupling measurements at these facilities is quite similar; in this paper, we refer to the LCF projections for definiteness. The LCF projections are based on full-simulation studies using the ILD detector model, with all relevant physics and beam-related backgrounds included. See [9, 10] for more details.

A question that is often asked about precision measurements is: What is the mass reach for the sensitivity to new particles? A simple estimate of the sensitivity can be derived from the idea that corrections to the Standard Model (SM) due to new heavy particles should be parametrized by higher-dimension operators in Standard Model Effective Field Theory (SMEFT). The leading such operators are at dimension 6, leading to an

estimate of the size of the corrections as

$$v^2/M^2 \sim 1\%, \quad (1)$$

where v is the Higgs field vacuum expectation value and M is the heavy particle mass, possibly suppressed further by a factor of α_w . However, (1) is only an order-of-magnitude estimate which might be modified by a large dimensionless prefactor. There are certainly beyond-SM theories that give small corrections to the Higgs couplings. A more meaningful question is whether there are opportunities for discovery with Higgs factory precision measurements [11]. To address this, it is necessary to study explicit models of new physics. This paper follows the approach of our earlier paper [12], applied now to a very different class of models.

It is well-known that Effective Field Theory descriptions of composite models of the Higgs boson such as the Strongly-Interacting Light Higgs (SILH) [13] can predict observable deviations in the Higgs couplings originating from physics at mass scales of 10 TeV and above. In this paper, we will address the mass reach of precision measurements in more explicit models of the Higgs boson in a composite state.

Observations at the LHC indicate that the 125 GeV Higgs boson has properties similar to those of an elementary scalar particle. A mechanism that makes this natural in the context of composite Higgs bosons is for the Higgs doublet fields to be a set of Nambu-Goldstone bosons associated with a strong interaction symmetry breaking at a high energy scale [14, 15]. Some explicit models that implement this idea are the Little Higgs models [16] or Natural Composite Higgs models [17, 18]. In models of Higgs as a Nambu-Goldstone boson, the high-energy theory has a large symmetry group G broken to a subgroup H by strong interaction effects. H would contain the electroweak $SU(2) \times U(1)$ as a subgroup. If H remained exact, the Higgs fields would be massless. However, the original theory could also include additional interactions that break G explicitly. Couplings to the electroweak interactions could provide some of these effects. It is still a problem if the perturbations induce quadratic divergences in the Higgs in one-loop diagrams. Little Higgs models avoid this issue using a mechanism called “collective symmetry breaking” [19]. In models implementing this mechanism, each individual weak coupling preserves enough symmetry that the Higgs is an exact Nambu-Goldstone boson and is forbidden from getting a mass. This happens, for example, in models of chiral symmetry breaking in which the left- and right-handed strongly interacting fermions have different weak interactions. It is not until two or more couplings are turned on simultaneously that the symmetry is broken sufficiently that the Higgs field acquires a mass and becomes a pseudo-Nambu-Goldstone boson (pNGB). Contributions to the Higgs mass involve these couplings collectively, and so the Higgs potential and the associated symmetry-breaking minimum appears in the second order of the perturbation expansion. This is an example of

a scenario in which an underlying symmetry-breaking at 10 TeV can feed down in two stages to a Higgs mass at the scale of 100 GeV.

In these models, signs of the physics of electroweak symmetry breaking appear in various different quantities that can be measured with high precision at Higgs factories. First, there is a modification of the top quark and bottom quark Yukawa couplings. Second, loop effects from heavy top quark partners shift the Higgs couplings, an effect most clearly visible in the couplings to W , Z , and gluons. Third, mixings of the top quark that play a role in the generation of the Higgs potential will typically modify the top quark electroweak couplings to the Z and W . A comprehensive exploration for signals of Higgs compositeness should include measurements of all of these observables.

Models in which electroweak symmetry breaking involves new interactions of the top quark must also satisfy another experimental constraint. Necessarily, from $SU(2) \times U(1)$ symmetry, the left-handed b quark must also have the new interactions. Then there is a danger that the Z boson decay width to the b will be altered, in conflict with the very precise measurement of

$$R_b = \frac{\Gamma(Z \rightarrow b\bar{b})}{\Gamma(Z \rightarrow \text{hadrons})}, \quad (2)$$

at the Z pole [20]. A realistic model must avoid this constraint. There are model-building solutions to the problem, for example, the imposition of a new custodial symmetry [21]. The models that we will study here respect this constraint.

In view of the considerations just described, we will study in this paper the effects on the Higgs boson and the top quark generated at 1-loop order in the Little Higgs model presented in [22]. This model is a variant of the model known as the “Littlest Higgs model” [23]. The strong-interaction symmetry breaking pattern is $G/H = SU(5)/SO(5)$. The Higgs fields are pNGBs in this coset space. The model contains only one quark with the quantum numbers of b_L , thus eliminating the possibility of mixing of the b_L with heavier states, the most important source of modification of the b_L coupling to the Z . The price of this is that the model has a larger than expected set of vectorlike top quark partners, including a partner with charge 5/3. All of these new fermions must have masses above about 1.2 TeV to avoid constraints from LHC searches. We choose this model to illustrate the effects that these vectorlike fermions can have on the Higgs boson and top quark properties when these are measured with high precision. Other Little Higgs models satisfying the constraints listed above will have similar effects on the Higgs boson and top quark sectors.

The structure of this paper is as follows: In Section II, we review the general structure of Little Higgs models and the specific properties of the $SU(5)/SO(5)$ just described. We also review the mechanism of collective symmetry breaking and explain how it gives rise to the top quark sector of the model. In Section III, we analyze

how this structure impacts the Higgs Yukawa couplings to fermions and bosons. In Section IV, we present the results of a complete scan of the parameter space of the model. This will illustrate the mass reach at which the influence of these heavy fermions can be observed in the precision measurements of Higgs Yukawa couplings. Section V discusses the influence of the heavy partners on the electroweak couplings of the top quark and illustrates the mass reach from the precision measurement of these couplings. This is a separate set of measurement that provides additional information on the physics of the vectorlike top quark partners. Section VI gives some conclusions.

II. ELECTROWEAK SYMMETRY BREAKING WITH HIGGS AS A PNGB

In this section, we review the elements of the Little Higgs model of Katz et al. [22]. This model is based on a strongly coupled field theory with the spontaneous symmetry breaking pattern $SU(5) \rightarrow SO(5)$. We remind the reader that this is the expected pattern of chiral symmetry breaking for a strongly coupled Yang-Mills theory with 5 elementary fermions in a real representation of a confining gauge group. We first give our description of the Nambu-Goldstone fields that arise from this breaking of the global symmetry. We then present the terms involving the fermions of the model, the top quark and its vectorlike partners. The mass terms and Yukawa couplings in this sector give the explicit $SU(5)$ symmetry breaking that will eventually lead to the nonzero Higgs potential and to the Higgs mass and vacuum expectation value.

A. $SU(5)/SO(5)$ Non-Linear Sigma Model

It is convenient to write the generators of $SU(5)$ in the **5** representation as 3×3 block matrices with blocks of size $(2, 1, 2)$, corresponding to an $SU(2) \times U(1) \times SU(2)$ subgroup of $SO(5) \in SU(5)$. In the model, The generators of the two $SU(2)$ subgroups are then written

$$Q_1^a = \begin{pmatrix} \sigma^a/2 & 0 & 0 \\ 0 & 0 & 0 \end{pmatrix}, \quad Q_2^a = \begin{pmatrix} 0 & 0 & -\sigma^{aT}/2 \\ 0 & 0 & 0 \end{pmatrix}. \quad (3)$$

the $U(1)$ generator is

$$Y = \frac{1}{2} \begin{pmatrix} \mathbf{1} & 0 & -1 \\ 0 & 0 & 1 \end{pmatrix}, \quad (4)$$

where $\mathbf{1}$ is the 2×2 unit matrix. In the model [22], the electroweak $SU(2)$ will be generated by $Q_1^a + Q_2^a$ and will be an exact symmetry at the level of the breaking of $SU(5) \rightarrow SO(5)$ symmetry breaking. The orthogonal generators $Q_1^a - Q_2^a$ will be spontaneously broken at this

level. From here on, we will refer to these as $SU(2)$ and $SU(2)'$, respectively.

We describe the breaking $SU(5) \rightarrow SO(5)$ by a symmetric 5×5 matrix whose vacuum expectation value is proportional to

$$\begin{pmatrix} 0 & 0 & \mathbf{1} \\ 0 & 1 & 0 \\ \mathbf{1} & 0 & 0 \end{pmatrix} \quad (5)$$

After symmetry breaking, the unbroken generators of $SU(5)$ are those that satisfy

$$T^a \Sigma_0 + \Sigma_0 T^{aT} = 0 \quad (6)$$

and the spontaneously broken generators satisfy

$$X^i \Sigma_0 - \Sigma_0 X^{iT} = 0. \quad (7)$$

The generators of $SU(2)$ belong to the unbroken subgroup.

Each NGB is associated with a broken generator. We can display these as a matrix $\Pi = \pi^a X^a$, given explicitly by

$$\Pi = \begin{pmatrix} \frac{\eta \mathbf{1}}{\sqrt{40}} + \frac{\theta^a \sigma^a}{\sqrt{8}} & \frac{h^T}{\sqrt{2}} & \phi \\ \frac{h^\dagger}{\sqrt{2}} & -\frac{2\eta}{\sqrt{10}} & \frac{\tilde{h}}{\sqrt{2}} \\ \phi^\dagger & \frac{h^\dagger}{\sqrt{2}} & \frac{\eta \mathbf{1}}{\sqrt{40}} - \frac{\theta^a \sigma^{aT}}{\sqrt{8}} \end{pmatrix} \quad (8)$$

where h is a complex $SU(2)$ doublet, and ϕ is a complex symmetric 2×2 matrix, that is, a complex $SU(2)$ triplet. In (8),

$$h = (h^+, h^0), \quad \tilde{h} = (-h^0, h^+) \quad (9)$$

The field η is a singlet that is also an exact NGB. This must be given mass, but it will not appear our analysis. If $SU(2)'$ is gauged, as it will be in this model, the fields θ^a will be eaten in the process of $SU(2)'$ mass generation.

Fluctuations along the broken directions included in (8) are encoded in Π and the non-linear sigma field

$$\Sigma(x) = e^{2i\Pi(x)/f} \Sigma_0. \quad (10)$$

Here f is the analog of the pion decay constant, with a value in the multi-TeV range. The kinetic term for the NGB fields in the Lagrangian is

$$\mathcal{L}_K = \frac{f^2}{4} \text{tr} |D_\mu \Sigma|^2. \quad (11)$$

with the coupling to the $SU(2) \times U(1)$ gauge fields

$$\begin{aligned} D_\mu \Sigma = \partial_\mu \Sigma - ig_j W_{\mu j}^a (Q_j^a \Sigma + \Sigma Q_j^{aT}) \\ - ig' B_\mu (Y \Sigma + \Sigma Y^T). \end{aligned} \quad (12)$$

		$SU(3)_c$	$SU(2)'$	$SU(2)$	$U(1)_Y$
X	p	3	1	2	$7/6$
	\tilde{t}	3	1	1	$2/3$
	\tilde{q}	3	2	1	$1/6$
\bar{X}	\tilde{q}	3	1	2	$-1/6$
	$\tilde{\bar{t}}$	3	1	1	$-2/3$
	\bar{p}	3	2	1	$-7/6$

TABLE I. Components of the vectorlike quark multiplets X and \bar{X} .

B. The top sector and the top quark Yukawa coupling

In the SM, the top quark is described by a left-handed $SU(2)$ doublet field $Q = (t_L, b_L)$ and left-handed singlet field $\bar{T} = \bar{t}_L$, the antiparticle of the t_R . In Little Higgs models, the quadratic divergence in the Higgs mass is cancelled by the contributions of vectorlike fermions arising from the strong interaction sector. In this model, we introduce left-handed fermions X and \bar{X} in the **5** and **5** of $SU(5)$, forming a set of heavy vectorlike quarks. The components of these multiplets— $(p, \tilde{t}, \tilde{q})$ and $(\bar{p}, \tilde{\bar{t}}, \tilde{\bar{q}})$, respectively—are listed in Table I, along with their quantum numbers under $SU(2)' \times SU(2) \times U(1)_Y$.

These assignments lead to fermion-Higgs Lagrangian terms

$$\mathcal{L}_t = \lambda_1 f \bar{X} \Sigma^\dagger X + \lambda_2 f \tilde{q} Q + \lambda_3 f \bar{T} \tilde{t} + \text{h.c.} \quad (13)$$

These terms produce vectorlike fermion masses and Yukawa couplings. It is convenient to write the mass matrix in the basis $(\bar{p}_t, \bar{t}, \tilde{\bar{q}}_t, \bar{T}) \times (p_t, \tilde{t}, \tilde{q}_t, Q_t)$. Before electroweak symmetry breaking, with $\langle h \rangle = 0$, this mass matrix takes the form

$$\begin{pmatrix} \lambda_1 f & 0 & 0 & 0 \\ 0 & \lambda_1 f & 0 & 0 \\ 0 & 0 & \lambda_1 f & \lambda_2 f \\ 0 & \lambda_3 f & 0 & 0 \end{pmatrix}. \quad (14)$$

This structure yields 3 massive charge $2/3$ quarks and one quark that remains massless at this level. This will be the physical top quark, which can gain mass only from electroweak symmetry breaking. The components of the physical top quark are given (as left-handed fermions) by

$$q_3 \equiv \frac{\lambda_2 \tilde{q} - \lambda_1 Q}{\sqrt{\lambda_1^2 + \lambda_2^2}}. \quad (15)$$

and

$$\bar{t} \equiv \frac{\lambda_3 \tilde{\bar{t}} - \lambda_1 \bar{T}}{\sqrt{\lambda_1^2 + \lambda_3^2}}. \quad (16)$$

They will obtain mass from a Yukawa coupling

$$\lambda_t h \bar{t} q_3 + \text{h.c.} \quad (17)$$

	p_t	\tilde{t}	\tilde{q}_t	Q_t
\bar{p}_t	$\lambda_1 f \cos^2 \theta$	$\lambda_1 f \frac{i}{\sqrt{2}} \sin 2\theta$	$-\lambda_1 f \sin^2 \theta$	0
$\tilde{\bar{t}}$	$\lambda_1 f \frac{i}{\sqrt{2}} \sin 2\theta$	$\lambda_1 f \cos 2\theta$	$\lambda_1 f \frac{i}{\sqrt{2}} \sin 2\theta$	0
$\tilde{\bar{q}}_t$	$-\lambda_1 f \sin^2 \theta$	$\lambda_1 f \frac{i}{\sqrt{2}} \sin 2\theta$	$\lambda_1 f \cos^2 \theta$	$\lambda_2 f$
T	0	$\lambda_3 f$	0	0

TABLE II. Full mass matrix for the charge $2/3$ fermions. In this table, $\theta = \langle h \rangle / (\sqrt{2} f)$.

with

$$\lambda_t = \frac{\lambda_1 \lambda_2 \lambda_3}{\sqrt{\lambda_1^2 + \lambda_2^2} \sqrt{\lambda_1^2 + \lambda_3^2}}. \quad (18)$$

After electroweak symmetry breaking, the mass matrix will take the form shown in Table II, with $\theta = \langle h \rangle / (\sqrt{2} f)$.

There are several points to note about this structure of the mass generation. First, the b_L remains massless at this stage of the analysis. Its mass will be supplied by additional, smaller, Yukawa terms. There is no other fermion with the same quantum numbers, before $SU(2) \times U(1)$ symmetry breaking, that can mix with it. Second, there is a vectorlike fermion in the theory with charge $5/3$. Thus the mass of this fermion does depend on h , and so it does not contribute to the Higgs boson properties through loop corrections. Finally, the generation of the top quark Yukawa coupling λ_t requires all three coefficients in (13) to be nonzero.

C. Higgs Potential from Collective Symmetry Breaking

To make explicit predictions from this theory, we will need the detailed formula for the Higgs potential. This is given by exchanges of the $SU(2)$ and $SU(2)'$ vector bosons within the strong interaction sector and loop corrections from the vectorlike top quark partners. This discussion follows closely the analysis in [22].

In the nonlinear sigma model description, the potential terms from $SU(2)$ and $SU(2)'$ vector boson exchange appear as quadratic divergences cut off at the scale f . These terms reflect the structure of an $SU(5)$ -invariant theory broken in order g^2 by weak gauging. The unique form is

$$V_{\text{gauge}}(\Sigma) = C g_j^2 f^4 \sum_a \text{tr} \left[(Q_j^a \Sigma) (Q_j^a \Sigma)^* \right] + C g'^2 f^4 \text{tr} \left[(Y \Sigma) (Y \Sigma)^* \right]. \quad (19)$$

We treat this as an order $g^2 f^2$ tree-level potential for h and ϕ . Expanding to quadratic order in ϕ and quartic

order in h gives

$$V_{\text{gauge}} = C g_1^2 f^2 \left| \phi_{ij} - \frac{i}{2f} (h_i h_j + h_j h_i) \right|^2 + C g_2^2 f^2 \left| \phi_{ij} + \frac{i}{2f} (h_i h_j + h_j h_i) \right|^2 + C g'^2 \left[f^2 \left(2 h_i^\dagger h_i + 4 \phi_{ij}^* \phi_{ij} \right) - \frac{1}{3} (h^\dagger h)^2 \right] \quad (20)$$

This yields a positive mass for the ϕ triplet,

$$m_\phi^2 = C (g_1^2 + g_2^2 + 4g'^2) f^2. \quad (21)$$

Notice the the Higgs doublet h receives a mass from (20), but only from the $U(1)$ boson exchange contribution. This mass term will be a relatively small contribution to the eventual full Higgs potential. The $SU(2)$ and $SU(2)'$ exchange terms each leave invariant $SU(3)$ symmetries that forbid a mass for the PNGBs and so cannot generate Higgs masses at this order. However, integrating out the ϕ fields generates an effective quartic coupling for the Higgs doublet,

$$\lambda = C \frac{4g_1^2 g_2^2 + \frac{11}{3}(g_1^2 + g_2^2)g'^2 - \frac{4}{3}g'^4}{g_1^2 + g_2^2 + 4g'^2}. \quad (22)$$

The 1-loop corrections to the potential (20) do generate Higgs mass terms, since these involve terms that break both $SU(3)$ global symmetries. These give the Higgs mass terms

$$\delta m_h^2 = \frac{9g^2 M_{W'}^2}{64\pi^2} \log \frac{\Lambda^2}{M_{W'}^2}. \quad (23)$$

from the W' exchanges, and

$$\delta m_h^2 = \frac{\lambda}{16\pi^2} M_\phi^2 \log \frac{\Lambda^2}{M_\phi^2}. \quad (24)$$

from the massive ϕ exchanges. Both of these effects are of order $g^4 f^2$. Note that all three Higgs mass terms that we have identified so far give rise to positive contributions to δm_h^2 .

The contribution of the top partners to the Higgs potential is generated at 1-loop order in the Yukawa couplings in (13) by the Coleman-Weinberg formula

$$\Delta V_{\text{CW}}^{(f)} = -\frac{3}{16\pi^2} \text{tr} \left(M_f(\Sigma) M_f^\dagger(\Sigma) \right)^2 \log \frac{M_f(\Sigma) M_f^\dagger(\Sigma)}{\Lambda^2} \quad (25)$$

where $M(\Sigma)$ is the mass matrix given in Table II. It is useful to have explicit expressions for the masses of the 3 heavy top quark partners. These are:

$$\begin{aligned} M_1 &= \lambda_1 f, \\ M_2 &= \left(a^2 + \frac{\lambda_t^2 \langle h \rangle^2 b^2}{a^2 - b^2} - \frac{\lambda_t^4 \langle h \rangle^4 (a^4 - a^2 b^2 + b^4)}{(a^2 - b^2)^3} \right)^{1/2}, \\ M_3 &= \left(b^2 - \frac{\lambda_t^2 \langle h \rangle^2 a^2}{a^2 - b^2} + \frac{\lambda_t^4 \langle h \rangle^4 (a^4 - a^2 b^2 + b^4)}{(a^2 - b^2)^3} \right)^{1/2}, \end{aligned} \quad (26)$$

with

$$a^2 = (\lambda_1^2 + \lambda_2^2) f^2, \quad b^2 = (\lambda_1^2 + \lambda_3^2) f^2. \quad (27)$$

For a generic set of Yukawa couplings, this expression (25) would yield a contribution to the Higgs mass of order $\lambda^2 f^2$, where here λ represents a Yukawa coupling. However, the charge 2/3 mass matrix exhibits a number of cancellations that are summarized as

$$0 = \frac{\partial}{\partial \theta} \text{Tr}[M^\dagger M], \quad (28)$$

$$0 = \frac{\partial}{\partial \theta} \text{Tr}[(M^\dagger M)^2]. \quad (29)$$

These implement the collective symmetry breaking. The first of these cancellations insures that the Higgs mass generated from the Coleman-Weinberg potential begins only in order $\lambda_t^4 f^2$. The second cancellation implies that this term is finite and not enhanced by a factor $\log(f^2/M^2)$. The explicit expression for the heavy quark contribution to the Higgs potential is

$$\begin{aligned} \delta V_{\text{eff}}(h) = & -\frac{3 \lambda_t^2}{8\pi^2} (h^\dagger h) \frac{a^2 b^2}{a^2 - b^2} \log \frac{a^2}{b^2} \\ & + \frac{3 \lambda_t^4}{16\pi^2} (h^\dagger h)^2 \left[\frac{(a^2 + b^2)}{(a^2 - b^2)^3} \right. \\ & \cdot \left. \left((3a^4 + 3b^4 - 4a^2 b^2) \log \frac{a^2}{b^2} - (a^4 - b^4) \right) \right. \\ & \left. + 2 \log \frac{ab}{h^2} \right]. \end{aligned} \quad (30)$$

The heavy top partner contribution to δm_h^2 is negative. This is a general feature of Little Higgs models, that integrating out the heavy quark partners generates a potential for the Higgs field with an instability to electroweak symmetry breaking. According to (18), the Yukawa couplings in (13) will be larger than the top quark Yukawa coupling $y_t = 1$, so this term easily overcomes the positive contribution to δm_h^2 from integrating out the heavy bosons. The required large size of the underlying Yukawa couplings will lead to large radiative corrections to Higgs couplings. This is possible even while these Yukawa couplings stay in the region in which they can be treated perturbatively.

III. MODIFICATION OF THE HIGGS BOSON COUPLINGS

By minimizing the potential computed in the previous section, and constraining the Higgs boson mass, the Higgs field vev, and the top quark mass to their measured values, we determine the allowed parameter space for the model [22]. Our next task is to compute the couplings of the Higgs boson over this parameter space and, in particular, the predicted deviations from their SM values. The modification of Higgs couplings in Little Higgs models

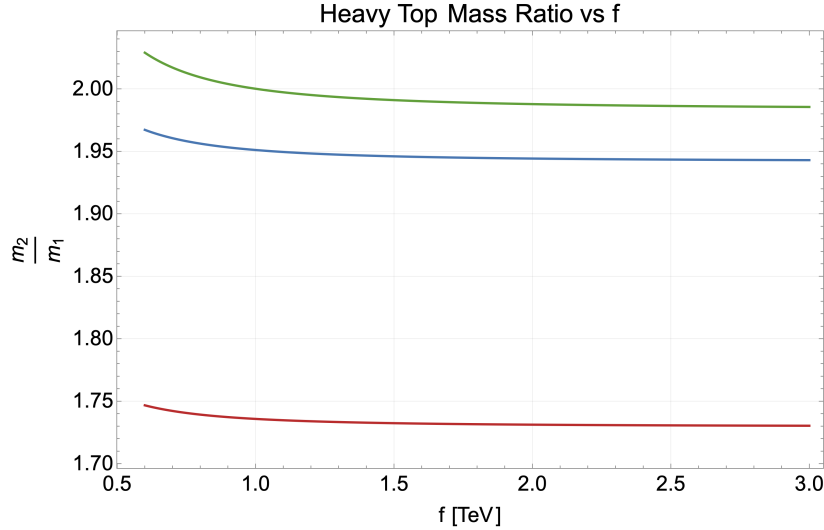


FIG. 1. The mass ratio of the first and second heavy top partners as a function of f . The three curves show the parameter choices, top to bottom: $\lambda_2/\lambda_3 = 1.3, 1.5, 1.7$.

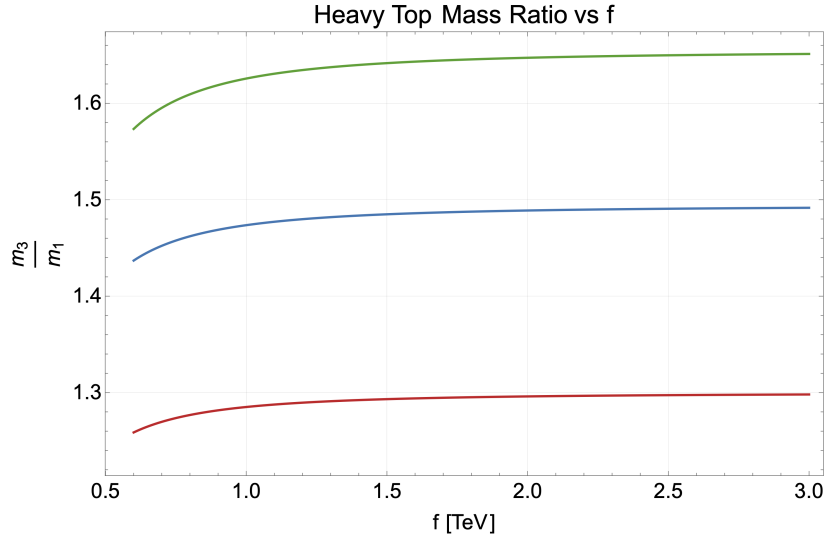


FIG. 2. The mass ratio of the first and third heavy top partners as a function of f . The three curves show the parameter choices, top to bottom: $\lambda_2/\lambda_3 = 1.3, 1.5, 1.7$.

has been studied some time ago by Han, Logan, McElrath, and Wang [24–26] and by Killian and Reuter [27].

In applying their analysis to this model, we follow the strategy of [26]. In that paper, the basic input parameters are taken to be the on-shell values of G_F , m_Z , α , and m_h . In this renormalization scheme, Higgs couplings receive a universal rescaling factor y_{G_F} and individual rescaling factors y_A for the $h \rightarrow A\bar{A}$ coupling. Then Higgs partial widths modified at the tree level are given by, for example,

$$\Gamma_b/\Gamma_b|_{SM} = y_{G_F^2}^2 y_b^2. \quad (31)$$

The partial width for $h \rightarrow gg$, which is generated at the

1-loop level, is given by the expression

$$\Gamma_g/\Gamma_g|_{SM} = y_{G_F^2}^2 \left| \frac{\sum_i y_i F_{1/2}(\tau_i)}{y_t F_{1/2}(\tau_t)} \right|^2, \quad (32)$$

where the index i runs over the top quark and its vector-like partners in the Little Higgs model, and $\tau = 4M_i^2/m_h^2$, and

$$F_{1/2}(\tau) = -2\tau \left[1 + (1 - \tau)f(\tau) \right], \quad (33)$$

with

$$f(\tau) = \begin{cases} \arcsin^2(1/\sqrt{\tau}), & \tau \geq 1, \\ -\frac{1}{4} \left[\log \frac{1+\sqrt{1-\tau}}{1-\sqrt{1-\tau}} - i\pi \right]^2, & \tau < 1. \end{cases} \quad (34)$$

The parameters y_A depend on the Yukawa couplings in (13) and also on the v and the value of the triplet vev through the parameter

$$x = \frac{2\lambda_{h\phi h}}{\lambda_{\phi^2}} \quad (35)$$

where $\lambda_{h\phi h}$ is the Higgs-triplet coupling and λ_{ϕ^2} is the scalar triplet coupling [25]. Points in the parameter space of the model must satisfy $x < 1$ for stability of the SM electroweak symmetry breaking pattern [26]. In the following, we will follow [26] in representing the couplings g_1 and g_2 by

$$c = \frac{g_1}{\sqrt{g_1^2 + g_2^2}} \quad s = \frac{g_2}{\sqrt{g_1^2 + g_2^2}}. \quad (36)$$

Evaluating the y_A for our model, we find, for the universal rescaling

$$y_{GF} = 1 + \left(-\frac{5}{24} + \frac{x^2}{8} \right) \frac{v^2}{f^2}, \quad (37)$$

for the bottom and top quark Yukawa couplings,

$$\begin{aligned} y_b &= 1 + \frac{v^2}{f^2} \left(-\frac{2}{3} + \frac{x}{2} - \frac{x^2}{4} \right), \\ y_t &= 1 + \frac{v^2}{f^2} \left(-\frac{2}{3} + \frac{x}{2} - \frac{x^2}{4} + \sum_i \frac{\lambda_1^2 \lambda_i^2}{(\lambda_1^2 + \lambda_i^2)^2} \right), \end{aligned} \quad (38)$$

where $i = 1, 2, 3$, and for the heavy top partners

$$y_{T_i} = -\frac{v^2}{f^2} \frac{\lambda_1^2 \lambda_i^2}{(\lambda_1^2 + \lambda_i^2)^2}. \quad (39)$$

The partial width for $h \rightarrow WW^*$ is affected not only by the coupling rescaling

$$y_W = 1 + \frac{v^2}{f^2} \left(-\frac{1}{6} - \frac{1}{4}(c^2 - s^2)^2 \right) \quad (40)$$

but also by shifts in the values of m_W , m_Z and $c_w = \cos \theta_w$ and $s_w = \sin \theta_w$ given by

$$\begin{aligned} y_{m_W}^2 &= 1 + \frac{v^2}{f^2} \left(-\frac{1}{6} - \frac{1}{4}(c^2 - s^2)^2 + \frac{1}{4}x^2 \right) \\ y_{m_Z}^2 &= 1 + \frac{v^2}{f^2} \left[-\frac{5}{12} + \frac{1}{2}x^2 \right] + \frac{m_W^2}{M_{Z_H}^2}, \\ y_{c_w}^2 &= 1 + \frac{v^2}{f^2} \frac{s_w^2}{c_w^2 - s_w^2} \left[-\frac{1}{4}x^2 \right] - \frac{s_w^2}{c_w^2 - s_w^2} \frac{m_W^2}{M_{Z_H}^2} \end{aligned} \quad (41)$$

In writing these formulae, we have taken account of the fact that the model includes only one gauged $U(1)$ group,

$U(1)_Y$. The M_{Z_H} term in the above equations is a consequence of the $SU(2)$ mixing, and having only the one gauged $U(1)_Y$ eliminates any M_{A_H} terms which arise in other equations in Appendix A of [26]. The partial width for $h \rightarrow WW^*$ is then given by

$$\Gamma_W/\Gamma_W|_{SM} = y_{GF}^2 \frac{y_{m_W}^2}{y_{m_Z}^2 y_{c_w}^2}. \quad (42)$$

These equations enable systematic studies of percent-level deviations in the Higgs couplings.

IV. SURVEY OF THE PARAMETER SPACE

We are now ready to present the main results of this paper, surveying the opportunities within the model of [22] for the discovery of deviations from the SM through high-precision measurement of the Higgs couplings.

Using the phenomenological formulae given above, we scanned the parameter space of the model in the following way: The model depends on the three coupling constants g_1 , g_2 , and g' , the three Yukawa couplings λ_1 , λ_2 , λ_3 , the pion decay constant f , and the 1-loop gauge potential parameter c in (19). Fixing the SM input parameters g , g' , v , and m_h and the top quark mass m_t then gives a 3-dimensional parameter space. We explored this space by varying values of the Yukawa couplings between 0 and 3, values of f up to 3 TeV (corresponding to strong interaction scales up to $4\pi f = 12$ TeV). We also scanned over the parameter C between 0.05 and 1 to find a value which allowed us to reproduce the observed values of the Higgs mass and vev. The value of the mixing angle s was scanned between 0.05 and 0.5, from which the values of g_1 and g_2 were calculated. These are primarily constrained by the parameter x . For each parameter set, we minimized the potential given in Sec. II C. To make this easier, we first computed v by balancing the fermionic contribution in (30) against the quartic Higgs interaction (22) and then treating the remaining terms as perturbative corrections. We then eliminated solutions violating the stability condition $x < 1$.

Using this strategy, it was difficult to find any points that give reasonable agreement with the known values of v and m_t . To overcome this difficulty, we carried out an initial random scan of the parameters using a very large number points. After finding a number of seed points that satisfied the constraints, we then carried out, for each of these, a random scan with 5% variation of the parameters. New solutions discovered in this way were used as new seed points, and so, eventually, we discovered extended parameter regions that satisfy the constraints. Having accumulated points in the parameter space in this way, we then used the formula of Sec. III to compute the expected deviations of the Higgs couplings.

In the space of solutions that we identified, the top partner masses generally have the relation

$$M_1 < M_3 < M_2. \quad (43)$$

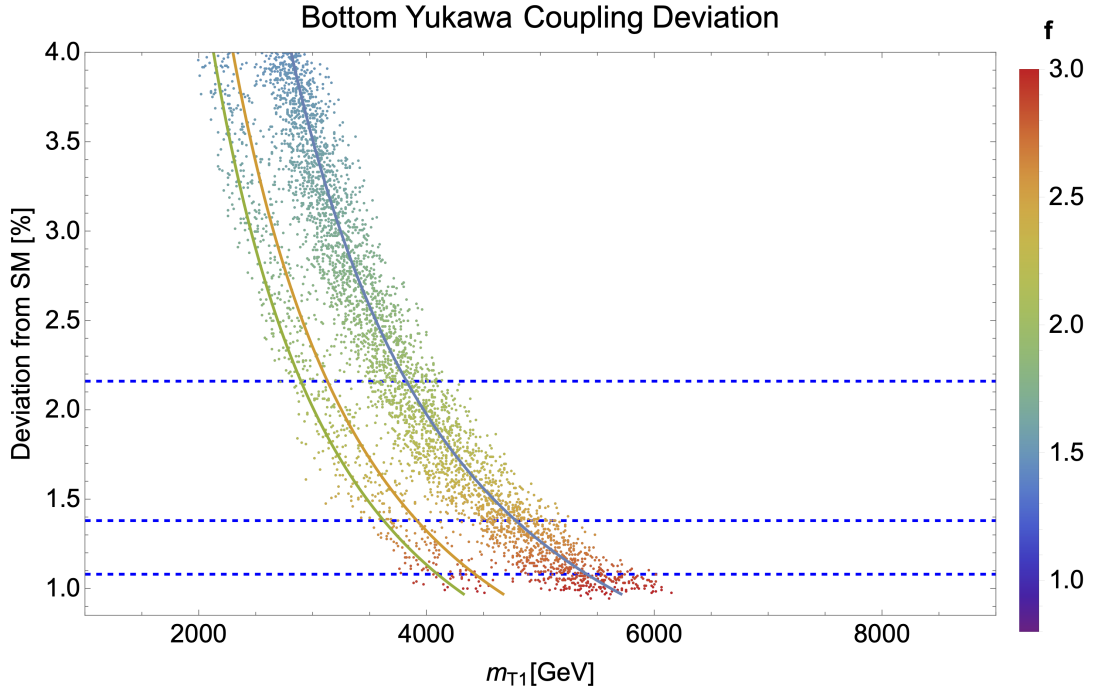


FIG. 3. Scatter plot depicting the percent change of the bottom quark Yukawa coupling from the SM value, over the parameter space of the Little Higgs model. The horizontal axis show the mass M_1 of the lightest top quark partner. The solid lines show the values in the three scenarios for the ratios of heavy partner masses $\lambda_2/\lambda_3 = 1.3, 1.5, 1.7$ shown in Figs. 1 and 2. The color of each point indicates the value of f . As in our study [12], the horizontal dotted lines show the lines of 3σ significance of three stages of the proposed LCF experimental program. The bottom of these lines is close to the 3σ significance value for FCC-ee and CEPC.

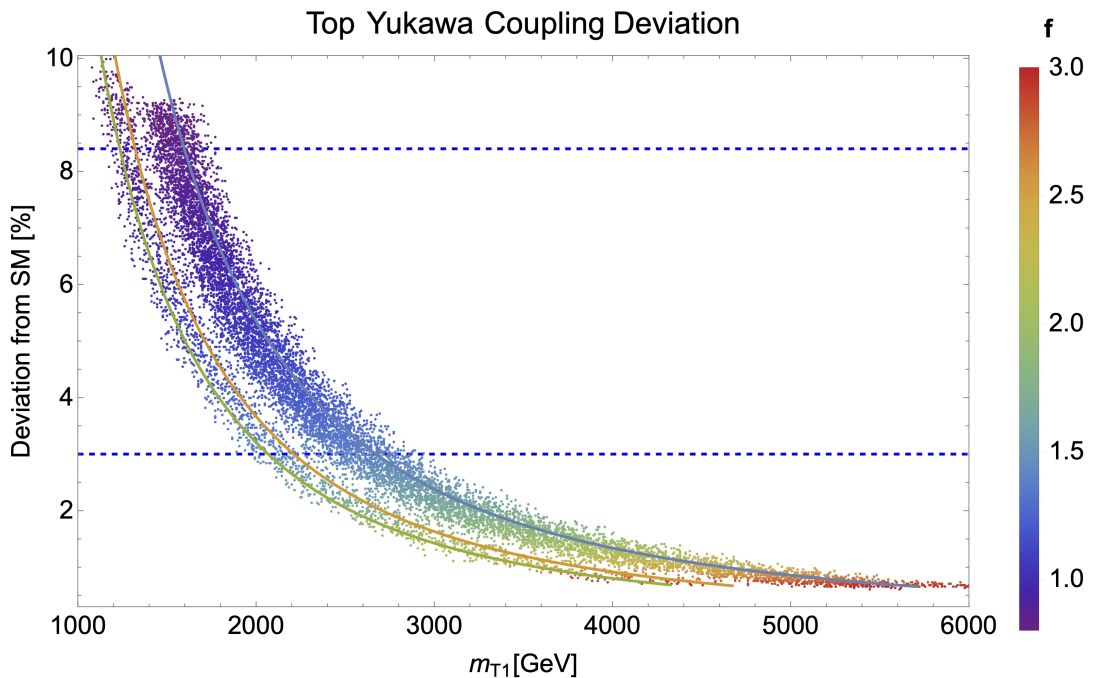


FIG. 4. Scatter plot depicting the percent change of the top quark Yukawa coupling from the SM value, over the parameter space of the Little Higgs model. The horizontal axis show the mass M_1 of the lightest top quark partner. The annotation of the plot is as in Fig. 3. In this case, only the lowest two horizontal lines are shown.

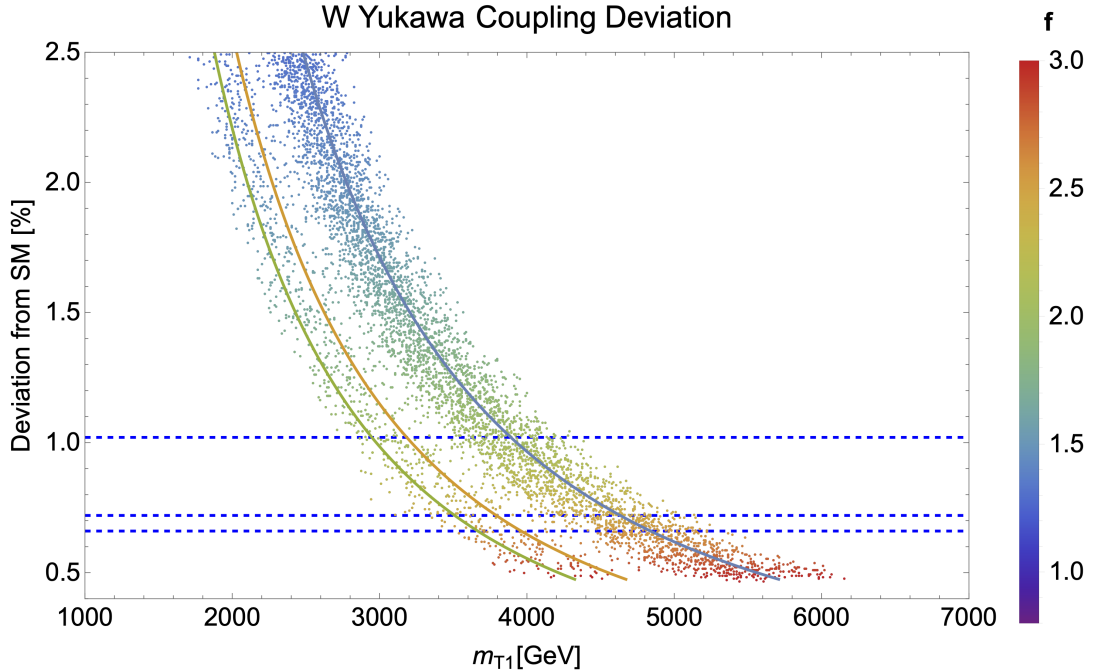


FIG. 5. Scatter plot depicting the percent change of the Higgs boson coupling to the W boson from the SM value, over the parameter space of the Little Higgs model. The horizontal axis show the mass M_1 of the lightest top quark partner. The annotation of the plot is as in Fig. 3.

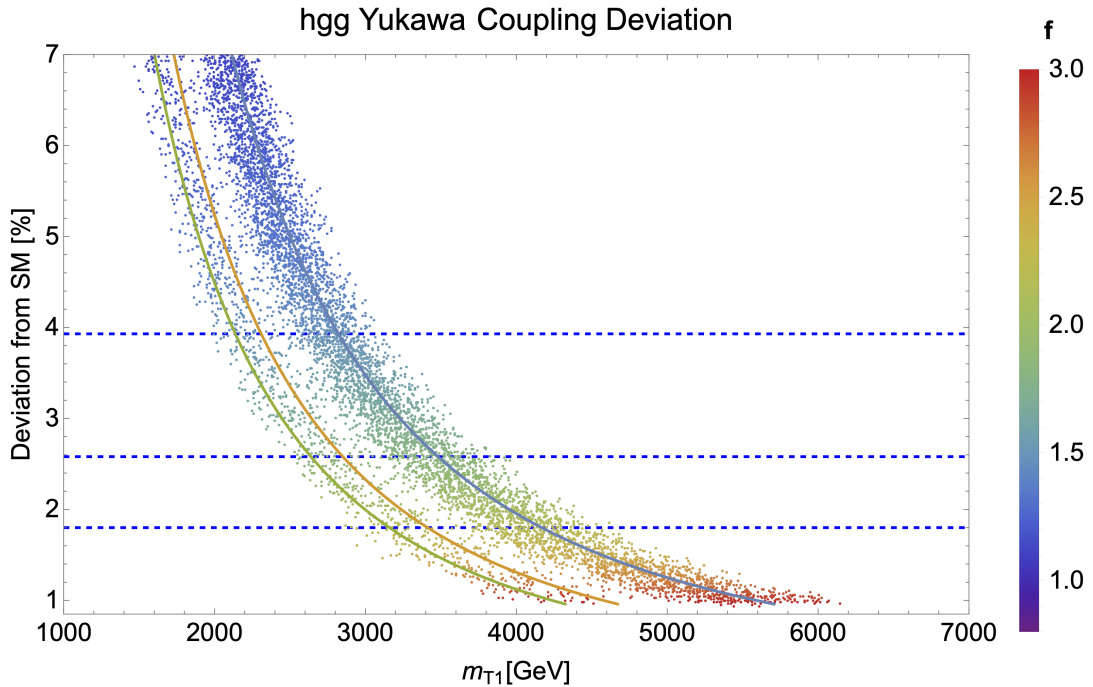


FIG. 6. Scatter plot depicting the percent change of the Higgs boson coupling to the gluon from the SM value, over the parameter space of the Little Higgs model. The horizontal axis show the mass M_1 of the lightest top quark partner. The annotation of the plot is as in Fig. 3.

Looking back at the formulae for these masses in (26), we see that the mass M_1 is highly correlated with the value of f . However, the solution space seems to divide into two distinct regions based on the mass ratio of the heavier partners M_3/M_2 . The dependence of the mass ratios on these parameters is shown in Figs. 1 and 2.

Our results for the Higgs coupling deviations are shown in Figs. 3-6. The two distinct regions of parameter space are clearly indicated. The upper bound of the allowed regions have the expected $1/M^2$ decoupling behavior. The solid lines correspond to the parameter choices for the Yukawa coupling ratio λ_2/λ_3 shown in Figs. 1 and 2. The horizontal lines indicate the expected 3σ significance expected from the successive stages of the LCF experimental program with data samples of 3 ab^{-1} at a CM energy of 250 GeV , 4 ab^{-1} at 550 GeV , and 8 ab^{-1} at 1000 GeV . The bottom line is very close to the 3σ expectations for the LCF with 4 ab^{-1} at 550 GeV and of the full FCC-ee and CEPC programs. For all of these facilities, the mass reach of the precision Higgs measurements of the individual Higgs couplings to b , W , and g indicates 3σ sensitivity to heavy top quark partners of $3\text{-}5 \text{ TeV}$. The combination of these measurements would give a discovery of well above 5σ significance. Please note that we have chosen to display the scan data against the lowest of the three top partner masses. There are models shown for which the value of M_2 to which these measurements are sensitive is greater than 10 TeV .

The measurement expectation for the top quark Yukawa coupling for LCF at 1000 GeV is a precision of 1% . This is essentially the same as the expectation for FCC-hh. This measurement does not seem to add much significance to the discovery in any model in this class.

V. MODIFICATION OF THE TOP QUARK ELECTROWEAK COUPLINGS

We noted in the Introduction that, in addition to modifications of the Higgs couplings, Little Higgs models will also modify the top quark coupling to the Z boson. Using the same scan that we have presented in the previous section, we can explore the size of this effect in the parameter space of the model [22].

The electroweak coupling modifications were also worked out in the general analysis presented in [25]. Specializing the formulae presented there to this model, we find for the left- and right-handed couplings of the b quark to the Z boson

$$g_L^b = \frac{g}{c_w} \left[\left(-\frac{1}{2} + \frac{1}{3} s_w^2 \right) - \frac{v^2}{f^2} \frac{c}{2s} c_w x_Z^{W'} \right] \\ g_R^b = \frac{g}{c_w} \left[\left(+\frac{1}{3} s_w^2 \right) \right], \quad (44)$$

and for the left- and right-handed couplings of the top

quark

$$g_L^t = \frac{g}{c_w} \left[\left(+\frac{1}{2} - \frac{2}{3} s_w^2 \right) - \frac{v^2}{f^2} \left(\frac{x_{L1}^2}{2} + \frac{x_{L2}^2}{2} - \frac{c}{2s} c_w x_Z^{W'} \right) \right] \\ g_R^t = \frac{g}{c_w} \left[\left(-\frac{2}{3} s_w^2 \right) \right], \quad (45)$$

where

$$x_{L1} = \frac{\lambda_1^2}{(\lambda_1^2 + \lambda_2^2)} \quad x_{L2} = \frac{\lambda_1^2}{(\lambda_1^2 + \lambda_3^2)}, \quad (46)$$

and $x_Z^{W'}$ is a correction due to the mixing of the two sets of $SU(2)$ bosons, given by

$$\frac{c}{2s} c_w x_Z^{W'} = -\frac{c^2(c^2 - s^2)}{4}. \quad (47)$$

This correction, equal and opposite for up and down quarks, is also present in the light quark couplings to the Z . The resulting shift of the b_L coupling then largely cancels out in the ratio R_b . The formulae of [25] also include larger corrections due to the mixing of the $SU(2)$ with heavy $U(1)$ bosons that are not present in the model that we consider here.

To compare to the capabilities of Higgs factories, we observe that our Little Higgs model gives no correction to the t_R coupling, while for the t_L coupling there is a fractional shift

$$\frac{\delta g_L^t}{g_L^t} = \frac{v^2}{f^2} \frac{x_{L1}^2 + x_{L2}^2 - c_w x_Z^{W'} \frac{c}{s}}{1 - (4/3)s_w^2}. \quad (48)$$

The values of this quantity over the parameter space of the model are shown in Fig. 7. The measurement of this quantity from $e^+e^- \rightarrow t\bar{t}$ is discussed in [8], which expects the precision

$$\frac{\delta g_L^t}{g_L^t} = 0.28\%, \quad (49)$$

from the LCF program at 550 GeV . The excellent sensitivity results from the fact that the cross section is dominated by s-channel γ and Z exchange. The two contributing amplitudes can be separated using beam polarization.

VI. CONCLUSIONS

In this paper, we have displayed the sensitivity of precision measurements at Higgs factories to an explicit model in which the Higgs boson is composite, realized as a Goldstone boson of a symmetry breaking at a high mass scale. Models of this type obey many constraints, from precision electroweak measurements and from direct searches for top quark partners and other heavy states that they include. Still, these models provide large parameter spaces in which ideas about the phenomenology

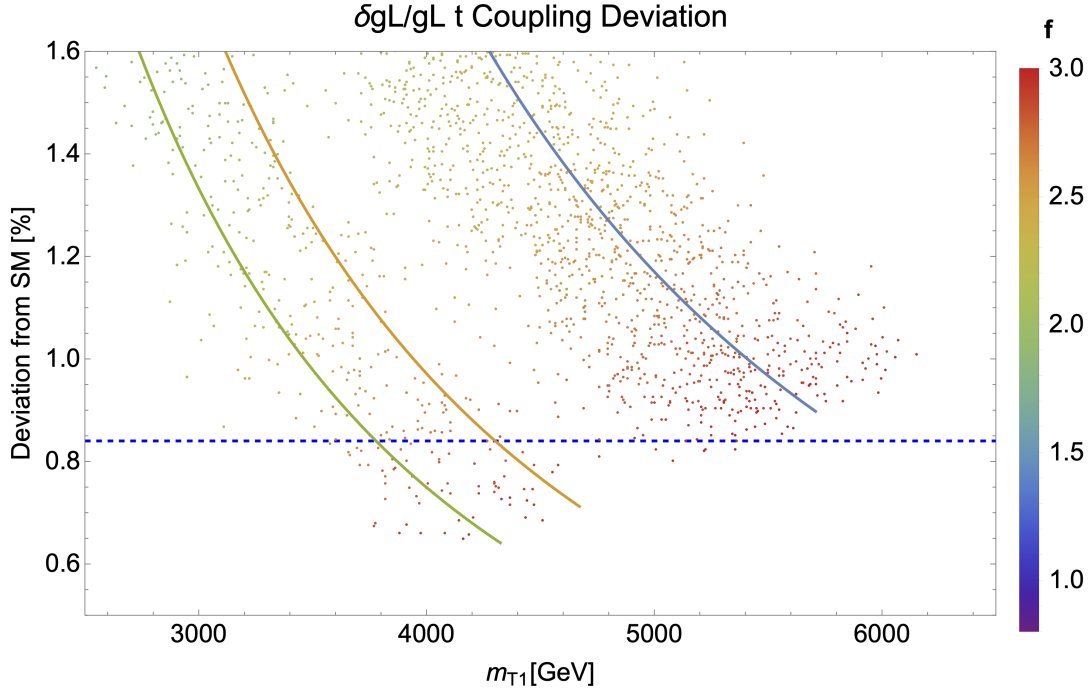


FIG. 7. Scatter plot depicting the percent change of the electroweak coupling of the t_L to the Z boson over the parameter space of the Little Higgs model. The horizontal axis show the mass M_1 of the lightest top quark partner. The annotation of the plot is as in Fig. 3. The single horizontal line is the line of 3σ significance from the LCF program at 550 GeV.

of these models can be tested. They are especially interesting as examples of models with large little hierarchies that appear naturally and point to physics goals beyond the reach of the LHC.

We have seen here that e^+e^- Higgs factories allow the observation of many signatures of these models, in the Higgs Yukawa couplings, in other Higgs couplings that the heavy particles of the theory influence through loop effects, and in the modification of the electroweak interactions of the top quark. This is only one of the many Beyond-Standard Model scenarios for which Higgs facto-

ries offer important opportunities for discovery.

ACKNOWLEDGMENTS

We continue to appreciate Ann Nelson's insights into the theory of electroweak symmetry breaking. We are grateful to Roman Pöschl and Marcel Vos for discussions of the measurement of top quark properties at Higgs factories. The work of KM and DGEW was supported in part by the grant NSF OIA-2033382. The work of MEP was supported by the US Department of Energy under contract DE-AC02-76SF00515.

[1] G. Aad *et al.* (ATLAS), Observation of a new particle in the search for the Standard Model Higgs boson with the ATLAS detector at the LHC, *Phys. Lett. B* **716**, 1 (2012), arXiv:1207.7214 [hep-ex].

[2] S. Chatrchyan *et al.* (CMS), Observation of a New Boson at a Mass of 125 GeV with the CMS Experiment at the LHC, *Phys. Lett. B* **716**, 30 (2012), arXiv:1207.7235 [hep-ex].

[3] *Snowmass White Paper Contribution: Physics with the Phase-2 ATLAS and CMS Detectors*, Tech. Rep. (CERN, Geneva, 2022).

[4] S. Dawson *et al.*, Report of the Topical Group on Higgs Physics for Snowmass 2021: The Case for Precision Higgs Physics, in *Snowmass 2021* (2022) arXiv:2209.07510 [hep-ph].

[5] A. Aryshev *et al.* (ILC International Development Team), The International Linear Collider: Report to Snowmass 2021, (2022), arXiv:2203.07622 [physics.acc-ph].

[6] H. Cheng *et al.* (CEPC Physics Study Group), The Physics potential of the CEPC. Prepared for the US Snowmass Community Planning Exercise (Snowmass 2021), in *Snowmass 2021* (2022) arXiv:2205.08553 [hep-ph].

[7] M. Benedikt *et al.* (FCC), Future Circular Collider Feasibility Study Report: Volume 1, Physics, Experiments, Detectors 10.17181/CERN.9DKX.TDH9 (2025), arXiv:2505.00272 [hep-ex].

[8] D. Attié *et al.* (Linear Collider Vision), A Linear Col-

lider Vision for the Future of Particle Physics, (2025), arXiv:2503.19983 [hep-ex].

[9] H. Abramowicz *et al.* (ILD Concept Group), International Large Detector: Interim Design Report, (2020), arXiv:2003.01116 [physics.ins-det].

[10] H. Ono and A. Miyamoto, A study of measurement precision of the Higgs boson branching ratios at the International Linear Collider, *Eur. Phys. J. C* **73**, 2343 (2013), arXiv:1207.0300 [hep-ex].

[11] M. E. Peskin, Model-Agnostic Exploration of the Mass Reach of Precision Higgs Boson Coupling Measurements, in *Snowmass 2021* (2022) arXiv:2209.03303 [hep-ph].

[12] K. Maayergi, D. G. E. Walker, and M. E. Peskin, Sensitivity of heavy Higgs boson to the precision Yukawa coupling measurements at Higgs factories, *Phys. Rev. D* **112**, 075032 (2025), arXiv:2506.16587 [hep-ph].

[13] G. F. Giudice, C. Grojean, A. Pomarol, and R. Rattazzi, The Strongly-Interacting Light Higgs, *JHEP* **06**, 045, arXiv:hep-ph/0703164.

[14] D. B. Kaplan and H. Georgi, SU(2) x U(1) Breaking by Vacuum Misalignment, *Phys. Lett. B* **136**, 183 (1984).

[15] D. B. Kaplan, H. Georgi, and S. Dimopoulos, Composite Higgs Scalars, *Phys. Lett. B* **136**, 187 (1984).

[16] M. Schmaltz and D. Tucker-Smith, Little Higgs review, *Ann. Rev. Nucl. Part. Sci.* **55**, 229 (2005), arXiv:hep-ph/0502182.

[17] E. Katz, A. E. Nelson, and D. G. E. Walker, The Intermediate Higgs, *JHEP* **08**, 074, arXiv:hep-ph/0504252.

[18] A. E. Nelson, M. Park, and D. G. E. Walker, Composite Higgs Models with a Hidden Sector, *Phys. Rev. D* **100**, 076015 (2019), arXiv:1809.09667 [hep-ph].

[19] N. Arkani-Hamed, A. G. Cohen, T. Gregoire, and J. G. Wacker, Phenomenology of electroweak symmetry breaking from theory space, *JHEP* **08**, 020, arXiv:hep-ph/0202089.

[20] S. Schael *et al.* (ALEPH, DELPHI, L3, OPAL, SLD, LEP Electroweak Working Group, SLD Electroweak Group, SLD Heavy Flavour Group), Precision electroweak measurements on the Z resonance, *Phys. Rept.* **427**, 257 (2006), arXiv:hep-ex/0509008.

[21] K. Agashe, R. Contino, L. Da Rold, and A. Pomarol, A Custodial symmetry for $Zb\bar{b}$, *Phys. Lett. B* **641**, 62 (2006), arXiv:hep-ph/0605341.

[22] E. Katz, J.-y. Lee, A. E. Nelson, and D. G. E. Walker, A Composite little Higgs model, *JHEP* **10**, 088, arXiv:hep-ph/0312287.

[23] N. Arkani-Hamed, A. G. Cohen, E. Katz, and A. E. Nelson, The Littlest Higgs, *JHEP* **07**, 034, arXiv:hep-ph/0206021.

[24] T. Han, H. E. Logan, B. McElrath, and L.-T. Wang, Loop induced decays of the little Higgs: $H \rightarrow gg$, gamma gamma, *Phys. Lett. B* **563**, 191 (2003), [Erratum: *Phys.Lett.B* 603, 257–259 (2004)], arXiv:hep-ph/0302188.

[25] T. Han, H. E. Logan, B. McElrath, and L.-T. Wang, Phenomenology of the little Higgs model, *Phys. Rev. D* **67**, 095004 (2003), arXiv:hep-ph/0301040.

[26] H. E. Logan, Littlest higgs boson at a photon collider, *Physical Review D* **70**, 10.1103/physrevd.70.115003 (2004).

[27] W. Kilian and J. Reuter, The Low-energy structure of little Higgs models, *Phys. Rev. D* **70**, 015004 (2004), arXiv:hep-ph/0311095.